Published in final edited form as:
J Neuropathol Exp Neurol. 2012 November ; 71(11): 959–972. doi:10.1097/NEN.0b013e31826f5876.

Differential Effects of FK506 on Structural and Functional Axonal Deficits Following Diffuse Brain Injury in the Immature Rat

Ann Mae DiLeonardi[1], **Jimmy W. Huh, MD**[3], and **Ramesh Raghupathi, PhD**[1,2]

[1]Program in Neuroscience, Drexel University College of Medicine, Philadelphia, PA 19129

[2]Department of Neurobiology and Anatomy, Drexel University College of Medicine, Philadelphia, PA 19129

[3]Department of Anesthesiology and Critical Care, Children's Hospital of Philadelphia, Philadelphia, Pennsylvania

Abstract

Diffuse axonal injury is a major component of traumatic brain injury in children and correlates with long-term cognitive impairment. Traumatic brain injury in adult rodents has been linked to a decrease in compound action potential (CAP) in the corpus callosum but information on trauma-associated diffuse axonal injury in immature rodents is limited. We investigated the effects of closed head injury on CAP in the corpus callosum of 17-day-old rats. The injury resulted in CAP deficits of both myelinated and unmyelinated fibers in the corpus callosum between 1 and 14 days post-injury (dpi). These deficits were accompanied by intra-axonal dephosphorylation of the 200-kDa neurofilament subunit (NF200) at 1 and 3 dpi, a decrease in total NF200 at 3 dpi and axonal degeneration at 3 and 7 dpi. Although total phosphatase activity decreased at 1 dpi, calcineurin activity was unchanged. The calcineurin inhibitor, FK506, significantly attenuated the injury-induced NF200 dephosphorylation of NF200 at 3 dpi and axonal degeneration at 3 and 7 dpi, but did not affect the decrease in NF200 protein levels or impaired axonal transport. FK506 had no effect on CAP deficits at 3 dpi, but exacerbated the deficit in only the myelinated fibers at 7 dpi. Thus, in contrast to adult animals, FK506 treatment did not improve axonal function in brain-injured immature animals, suggesting that calcineurin may not contribute to impaired axonal function.

Keywords

Axonal Injury; Calcineurin; Compound action potential; FK506; Immature rat; Neurofilament; Traumatic brain injury

INTRODUCTION

Traumatic brain injury (TBI) is a leading cause of death in infants and children and results in long-lasting cognitive deficits in survivors (1, 2). The primary pathologic process in brain-injured children is diffuse axonal injury, which has correlates with long-term negative

Send correspondence and reprint requests to: Ramesh Raghupathi, PhD, Department of Neurobiology and Anatomy, Drexel University College of Medicine, 2900 Queen Lane Philadelphia, PA 19129. Tel: 215-991-8405; Fax: 215-843-9082; rramesh@drexelmed.edu.

cognitive outcome (3-5). Diffuse axonal injury in animals is manifested as traumatic axonal injury (TAI), which results from a combination of mechanoporation of the axolemma, focal loss of microtubules, ionic dysregulation, impaired axonal transport and neurofilament compaction (6-12). Axonal swellings containing accumulations of amyloid precursor protein (APP), synaptophysin or compacted neurofilaments, and retrograde tracer studies provide evidence of TAI in multiple white matter tracts of adult brain-injured animals (12-15). We and others have shown that traumatic injury to the immature brain results in TAI that is manifest as axonal swellings containing APP or neurofilaments (16-20). Over time, the injured axons undergo secondary axotomy and degeneration (21, 22), which occurs in both immature (19) and adult animals (13).

TAI in adult rodents has been linked to functional deficits observed as a decrease in compound action potential (CAP) within the corpus callosum and cerebellum (13, 23-25). CAPs across the corpus callosum are characterized by a 2-peak waveform that represents the field potential of myelinated axons and unmyelinated axons (26). Myelinated and unmyelinated fibers can be identified based on recruitment (threshold of activation), refractoriness (minimum time between 2 action potentials), and susceptibility to 4-aminopyridine (4-AP), which increases the duration and amplitude of unmyelinated axons but has no effect on myelinated axons (26). Diffuse brain injuries in adult rats result in deficits in CAP of both myelinated and unmyelinated axons at 1 day. Although the myelinated axons recover by 7 days, deficits are sustained in unmyelinated fibers (23, 24, 27). In contrast to these observations, concussive brain injury in adult mice led to a lasting decrease (up to 14 days) in CAP of myelinated fibers, suggesting that there are species differences (13). Because there have been no studies evaluating axonal function following diffuse brain trauma in immature rodents, our first goal was to determine the effect of closed head injury on CAP in the corpus callosum of the 17-day-old rat.

Increased calcium entry into axons has been suggested as a potential mechanism underlying both CAP deficits and TAI (8, 28-31). Inhibition of either calpain (a calcium-activated protease) or calcineurin (a calcium-dependent phosphatase) has been successful in attenuating CAP deficits as well as axonal injury following diffuse brain injury in the adult rat (27, 32, 33). TBI in the immature rat leads to neurofilament compaction (16), which may result from proteolysis (via calpain) or dephosphorylation (via calcineurin) of the side-arm domains of neurofilament subunits (34-36). Diffuse brain injury or optic nerve stretch in adult rats resulted in dephosphorylation of the 200-kDa neurofilament subunit (37-39), implicating calcineurin, which can dephosphorylate neurofilaments (40, 41), and is increased following TBI (42-45). Moreover, the calcineurin inhibitors FK506 and cyclosporin-A have been reported to reduce the burden of axonal injury following diffuse brain trauma in adult animals (32, 33, 46-49), and to decrease neurofilament disruption following axon stretch in vitro (50). Our previous observations of neurofilament compaction in axonal swellings in the injured immature rat brain led us to determine whether axonal neurofilaments would undergo dephosphorylation and to hypothesize that FK506 would limit the extent of neurofilament dephosphorylation and reverse CAP deficits following diffuse brain trauma in immature rats.

MATERIALS AND METHODS

Brain Injury

Seventeen-day-old male and female Sprague-Dawley rat pups (Charles River Laboratories, Wilmington, MA; 33 ± 4 g, mean ± SD) were anesthetized with isoflurane (5%) and subjected to diffuse brain injury, as previously described (19). Sham-injured animals were anesthetized and surgically prepared but did not receive an injury. The animals used to characterize the alterations in axonal conductance and neurofilament expression are listed in

Table 1; those used for the characterization of the temporal alterations in neurofilament dephosphorylation were part of a larger study evaluating histopathological alterations and behavioral deficits following diffuse head injury in immature rats (19). In the experiments evaluating the effect of FK506, brain-injured animals received i.p. injections of vehicle (20% methanol in 1X PBS), 10 or 25 mg/kg FK506 (AG Scientific, San Diego, CA), immediately and 6 hours following injury (Table 2). In preliminary studies, 1 and 5mg/Kg doses were tested based on efficacy reported in previous studies (33, 46, 47, 51); however, because of a lack of effect of these doses on neurofilament dephosphorylation and intra-axonal accumulation of APP, the doses listed above were tested. All surgical procedures were done in accordance with the rules and regulations of the Institutional Animal Care and Use Committee of Drexel University College of Medicine and were in compliance with the Guide for the Care and Use of Animals. Animals were placed on a heating pad to maintain body temperature at 37°C throughout the procedures and recovery.

CAP Measurements

Animals were anesthetized, brains rapidly removed, and 450-μm-thick coronal slices containing the corpus callosum were prepared as described by Reeves et al (23) (Fig. 1A). Evoked CAPs were recorded across the corpus callosum (Fig. 1B) using an Axoclamp 2B amplifier, digitized at 100 kHz, and stored on disk for analysis. Constant current pulses (200 μs duration) were used to evoke CAPs in the corpus callosum and the current where the CAP reached its maximum was defined as the maximum current for each individual slice; intensity of the current was decreased by 5 100-μA steps to construct input-output curves. The amplitude of the N1 component of the CAP (representing myelinated fibers) was quantified as the difference from the first positive peak to the first negative peak (Fig. 1C). To determine the amplitude of the N2 component (representing unmyelinated fibers), an arbitrary line was drawn relative to baseline and a tangent dropped to the second negative peak (Fig. 1C). Duration was determined as the time from the first to the second positive peak for the N1 component and from the second positive peak until the waveform reached baseline for the N2 component (Fig. 2C). Conduction velocity was calculated using the distance between the recording and stimulating electrodes as a function of the time from the stimulus artifact to the negative peak of N1 or N2. To analyze refractoriness (a measure of the time required to depolarize the membrane from a hyperpolarized state into a range where a second action potential can be generated), pairs of pulses were used where the interpulse interval increased in 0.5-msec steps from 3 msec through 12 msec, then in 5-msc steps from 15 msec through 35 msec at the maximum current determined from the input-output testing for each slice. The amplitude of the peak from the second pulse, calculated as a percent of the peak from the first pulse, was plotted as a function of the interpulse interval. From this, the interval at which the amplitude recovered to 50% of the first peak was determined and compared across groups. All quantitative analysis of electrophysiology was performed on waveforms that were the average of 4 successive sweeps; 2 slices per animal were averaged to generate a single value for that animal.

Immunohistochemistry and Histology

Animals were perfused and brains were processed as previously described (19). Sets of sections were stained for dephosphorylated 200-kDa neurofilament subunit (clone SMI-32, 1:5000, Sternberger Monoclonals, Baltimore, MD) or total 200-kDa neurofilament proteins (clone N52, 1:5000, Sigma-Aldrich, St. Louis, MO) and detected using biotinylated donkey anti-mouse IgG secondary antibody (1:500, Jackson ImmunoResearch, West Grove, PA) with diaminobenzidine as the chromogen. Double-label immunofluorescence for dephosphorylated neurofilament and APP was performed as previously described (16). Degeneration of axons was evaluated using Fluoro-Jade B (19).

SMI-32 and NF200 immunoreactivity were quantified at 3 levels (2.8, 3.6, and 4.3 mm posterior to bregma) using the grid method, as described (16). The area of APP immunoreactivity in the subcortical white matter regions was also measured in these levels using Image J (National Institute of Health), and expressed as a function of the total area of the coronal slice; each animal was represented by 1 value that was the average of the 3 sections. To quantify axonal degeneration, Matlab (version R010b) was used to calculate the density of Fluoro-Jade B-positive profiles in the corpus callosum in 3 sections taken from 2.8, 3.6, and 4.3 mm posterior to bregma. Using the image toolbox, profiles were first identified based on staining intensity relative to background. Profile edges were defined based on a 40% increase from the immediate background with profiles containing between 4 and 350 pixels deemed positive. The number of profiles in each section was determined as a function of the area of the corpus callosum in that section and the final value represented the average profile density across the 3 sections.

Immunoblot Analysis

Lysates of subcortical white matter was prepared as described (13). Samples were run on denaturing 7.5% polyacrylamide gels, transferred to PVDF membranes that were probed with anti-NF200 (clone N52, 1:10,000) and detected using donkey anti-mouse IgG conjugated to horseradish peroxidase with enhanced chemiluminescence (ECL, Amersham, Arlington, IL). Equal loading of protein was confirmed by reprobing the blots with an antibody to actin (clone AC-40, 1:1000, Sigma-Aldrich). Densitometric analysis was performed by normalizing the intensity of the band of interest to that of actin (normalized relative optical density, ROD), using GeneSnap imaging and software (SynGene, Frederick, MD). Each sample was evaluated at least twice.

Calcineurin Activity

Lysates of subcortical white matter and cortex were prepared as described from sham- and brain-injured animals at 1 and 3 days post-injury (dpi) (13). Total phosphatase and calcineurin activities were assayed using a kit (Enzo Life Sciences, Farmingdale, NY) according to the manufacturer’s instructions.

Statistical Analysis

All data are presented as means ± SD. For quantification of amplitudes of the CAP, a mixed design ANOVA was utilized with injury and time as between-subject comparisons and normalized stimulus current as repeated measure factor using Statistica (version 7.1, Statsoft, Tulsa OK). All other data were compared using a factorial ANOVA with either injury status and time post-injury or treatment and time post-injury as between-subject comparisons. Post-hoc analysis was performed using the Newman-Keuls test. A p value of less than 0.05 was considered significant in all analyses.

RESULTS

Acute Neurologic Outcomes following Diffuse Brain Injury

Closed head injury in 17-day-old rats resulted in skull fractures and hematomas that were accompanied by a brief period (4-8 seconds) of apnea (Tables 1, 2), similar to earlier observations (19). Importantly, no differences in body weights and post-traumatic apnea times were observed between the groups assigned for the various outcomes (Tables 1, 2).

Compound Action Potential following Diffuse Brain Injury

Evoked CAPs in the corpus callosum of sham-injured immature (1, 7, and 14 dpi) rats resulted in a biphasic waveform similar to that observed in uninjured adult rats and mice

(13, 23). The amplitude of the myelinated fibers (N1) of the CAP was consistently larger than that of the unmyelinated fibers (N2) (Fig. 2A). The amplitude of the N1component remained constant over the 3 ages analyzed (Fig. 2B, C; $F(2, 38) = 0.601$, $p > 0.5$), whereas the amplitude of the N2 component decreased with age (Fig. 2D, E; TIME effect, $F(2, 37) = 4.54$, $p < 0.02$), suggestive of an increase in the degree of myelination. Diffuse brain injury resulted in a change to the shape of the waveform of CAPs whereby both N1 and N2 components became temporally closer and the signal rarely returned to baseline between the 2 peaks (Fig. 2A). Quantitative analysis revealed a decrease in the amplitude of both N1 (Fig. 2B, C; INJURY effect, $F(1, 38) = 71.83$, $p < 0.0001$) and N2 components (Fig. 2D, E; INJURY effect, $F(1, 37) = 5.16$, $p < 0.03$). The absence of an interaction effect (TIME × INJURY) for both N1 ($F(2, 38) = 1.62$, $p > 0.05$) and N2 ($F(2, 37) = 0.91$, $p > 0.05$) components indicate sustained deficits in the CAP amplitudes. Furthermore, slices from brain-injured animals required significantly more current to reach the maximum response vs. slices from sham-injured animals (1 day: 1117 ± 509 μA vs. 875 ± 160 μA; 7 days: 1080 ± 239 μA vs. 849 ± 130 μA; 14 days: 975 ± 323 μA vs.725 ± 83 μA; INJURY effect: $F(1, 37) = 8.37$, $p < 0.007$).

Brain injury resulted in a decrease in the duration of both the N1 (Fig. 3; INJURY effect, $F(1, 37) = 59.88$, $p < 0.0001$) and N2 components (Fig. 3B; INJURY effect, $F(1, 37) = 17.41$, $p < 0.005$) of the CAP over the 14 dpi period. The conduction velocity of the N1 component increased with age (Fig. 3C; TIME effect, $F(2, 34) = 3.43$, $p < 0.05$), and was unaffected by injury (Fig. 3C; $F(2, 34) = 3.23$, $p > 0.05$). In contrast, the conduction velocity of the N2 component was independent of age (Fig. 3D; $F(2, 342) = 0.18$, $p > 0.05$), but was significantly increased in slices from brain-injured rats vs. those from sham-injured animals (Fig. 3D; INJURY effect, $F(2, 34) = 13.92$, $p < 0.001$). Analysis of paired pulse recordings revealed that neither age nor injury affected the refractoriness of the N1 component (Fig. 3E). Although age did not affect the refractoriness of the N2 component (Fig. 3F; $F(2, 32) = 154$, $p > 0.05$), an INJURY effect was observed (Fig. 3F; $F(1, 32) = 17.79$, $p < 0.001$. The decrease in refractoriness of the N2 component was dependent on age post-injury (TIME × INJURY, $F(2, 32) = 5.40$, $p < 0.01$), and was significant at 1 and 14 dpi (Fig. 3F, $p < 0.05$).

Neurofilament Dephosphorylation following Diffuse Brain Injury

Immunoreactivity for dephosphorylated 200-kDa neurofilament protein was not observed in white matter tracts of sham-injured animals, (Fig. 4A). Diffuse brain injury resulted in swollen axons containing dephosphorylated neurofilaments in the corpus callosum, cingulum and lateral white matter tracts between the cingulum and the rhinal fissure (Fig. 4B, C); injured axons were present between bregma and 5.6 mm posterior to bregma. Immunoreactivity for the SMI-32 antibody was extensive at 1 and 3 dpi in the corpus callosum (Fig. 4B, C), cingulum, and lateral white matter tracts (data not shown) and was present in swollen, contiguous axons (Fig. 4D), some of which ended in terminal bulbs indicative of axonal disconnection (Fig. 4E, F). By 7 dpi, only a few injured axons were visible (data not shown). Axonal SMI-32 immunoreactivity was present in the areas of the white matter tracts in which APP-positive swellings (19) and neurofilament compaction (16) have been observed following brain injury. Although the majority of axonal swellings that stained for SMI-32 did not stain for APP (arrows, Fig. 4G-I), there were sporadic axonal swellings that stained for both SMI-32 and APP (arrowheads, Fig. 4G-I). Sham-injured animals had no axons that stained for either APP or SMI-32 (data not shown).

Immunoreactivity for total NF200 was observed in the white matter tracts in sham-injured animals and appeared as diffuse staining within axons at all 3 ages evaluated (Fig. 5A). Following injury, axonal accumulations of NF200 were observed in the corpus callosum, cingulum, and lateral white matter tracts at 1 dpi (Fig. 5B) and 3 dpi (Fig. 5C), predominantly as terminal bulbs; by 7 dpi, NF200-positive axonal swellings were minimally

observed (data not shown). Interestingly, the overall NF200 immunoreactivity in contiguous axons appeared to decrease by 3 dpi (Fig. 5C), which was confirmed using immunoblot analysis of white matter tissue lysates (Fig. 5D). Total NF200 appeared as doublet ranging in size between 180 and 200 kDa, as previously observed (52) (Fig. 5D), and quantification of ROD of both bands representing total NF200 protein revealed an increase in NF200 expression as a function of age in the sham animals (Fig. 5E; TIME effect, $F(2, 29) = 6.92$, $p < 0.005$), and a decrease as a function of INJURY (Fig. 5E; $F(1, 29) = 11.99$, $p < 0.005$).

Calcineurin Activity following TBI

Diffuse brain trauma resulted in a decrease in total phosphatase activity in lysates of white matter at 1 dpi, but not 3 dpi (Fig. 6A; $F(2, 10) = 5.74$, $p < 0.05$); however, there was no change in the calcineurin activity (Fig. 6A; $F(2, 10) = 2.49$, $p > 0.05$). Neither total phosphatase nor calcineurin activity in cortical lysates was affected by brain trauma (Fig. 6B).

Effect of FK506 on Post-traumatic Neurofilament Dephosphorylation

Brain trauma in the rats given vehicle resulted in intra-axonal SMI-32-positive swellings at 1 and 3 dpi in the corpus callosum (Fig. 7A, 7B) and cingulum (not shown) to a similar extent as in untreated brain-injured animals. Administration of 10 or 25 mg/kg of the calcineurin inhibitor, FK506, had no effect on neurofilament dephosphorylation at 1 dpi (Fig. 7C), but reduced the extent of SMI-32 immunoreactivity at 3 dpi (Fig. 7D). Quantification of SMI-32-positive profiles revealed significantly fewer profiles in FK506-treated animals vs. vehicle-treated animals (Fig. 7E; TREATMENT effect, $F(2, 31) = 14.64$, $p < 0.0005$). An interaction effect (TIME × TREATMENT, $F(2, 31) = 7.55$, $p < 0.005$) revealed the effect of FK506 was only apparent at the 3 d time point at both doses (Fig. 7E, $p < 0.001$). Similarly, NF200 examined at 3 dpi following administration of either vehicle (F) or FK506 (25 mg/kg) also showed a reduction in the extent of NF200-positive profiles. Quantification of NF200-positive profiles revealed there were significantly fewer profiles in the FK506-treated vs. vehicle-treated animals (Fig. 7H; TREATMENT effect, $F(1,9) = 6.33$, $p < 0.05$. Analysis of neurofilament expression at 3 dpi using immunoblots revealed an injury-induced decrease in total NF200 (Fig. 7I, J; INJURY effect, $F(1, 11) = 6.33$, $p > 0.001$); treatment with FK506 (25mg/kg) had no effect (Fig. 7I, J; TREATMENT effect, $F(1, 11) = 1.43$, $p > 0.05$). No changes in neurofilament phosphorylation or expression were observed in sham-injured animals receiving FK506 (data not shown).

Effect of FK506 on Post-traumatic Axonal Degeneration

Diffuse brain injury resulted in intra-axonal accumulation of APP within multiple white matter tracts at 1 and 3 dpi (Fig. 8A, C). In contrast to observations in adult brain-injured rats, post-traumatic administration of FK506 did not affect the extent of impaired axonal transport in the corpus callosum at any time post-injury (Fig. 8B, D). These qualitative observations were confirmed by quantification of the area positive for APP immunoreactivity in the subcortical white matter region. Factorial ANOVA revealed a TIME effect indicative of decreased APP immunoreactivity at 3 dpi ($F(1, 33) = 48.84$, $p < 0.0001$) but not a TREATMENT effect, suggesting that administration of neither dose of FK506 reduced axonal injury at either time point ($F(2, 33) = 1.79$, $p > 0.1$) (Fig. 8E). As reported previously (19), areas immunoreactive for axonal APP at 1 and 3 dpi demonstrated evidence of axonal degeneration (Fluoro-Jade B reactivity) at 3 and 7 dpi (Fig. 8F, H). Post-traumatic administration of FK506 reduced the extent of Fluoro-Jade B reactivity in the corpus callosum (Fig. 8G, 8I). Quantification of the density of Fluoro-Jade B-positive profiles revealed a treatment effect (Fig. 8J; $F(1, 19) = 8.21$, $p < 0.001$). Administration of FK506 to sham-injured animals did not result in intra-axonal APP accumulation or axonal degeneration (data not shown).

Effect of FK506 on Compound Action Potential

At 3 and 7 dpi, the amplitudes of both N1 and N2 components of the CAP were decreased in vehicle-treated (20% methanol in 1X PBS) brain-injured rats (Fig. 8K, L) to a similar extent as in sham control rats (Fig. 2C, E). Although administration of FK506 (25 mg/Kg) was observed to reduce the extent of neurofilament dephosphorylation and axonal degeneration (vide supra), it decreased the amplitude of the N1 component compared to vehicle-treated animals (Fig. 8K; TREATMENT effect, $F(1, 18) = 10.33$, $p < 0.005$). In addition, an interaction effect (TREATMENT × TIME, $F(1,18) = 5.97$, $p < 0.05$) revealed that the FK506-induced decrease in amplitude was restricted to the 7-day time point (Fig. 8K). No effect of post-traumatic administration of FK506 was observed on the amplitude of the N2 component of the CAP at either 3 or 7 dpi, although the amplitude did increase between 3 and 7 dpi independent of treatment status (TIME effect, $F(1, 18) = 9.21$, $p < 0.01$). Treatment of brain-injured animals with FK506 did not affect any of the other parameters of the CAP such as duration and conduction velocity (data not shown). Administration of FK506 to sham-injured rats did not affect axonal conductance (data not shown).

DISCUSSION

This is the first study characterizing deficits in compound action potentials following traumatic brain injury in the immature rat. The decrease in CAP amplitude of both the myelinated and unmyelinated fiber populations was observed as early as 1 dpi and persisted up to 2 weeks. These functional deficits were accompanied by intra-axonal dephosphorylation of NF200, a decrease in total NF200 protein, and axonal degeneration. Treatment with the calcineurin inhibitor, FK506 significantly attenuated intra-axonal accumulations of total and dephosphorylated NF200 and axonal degeneration. FK506 had no effect on NF200 protein expression or CAP deficits at 3 dpi, but it exacerbated the CAP deficit in only the myelinated fibers at 7 dpi. These data do not appear to provide a causal link between post-traumatic neurofilament alterations and axonal conductance and underscore the importance of using multiple outcome measures to evaluate efficacy of a treatment paradigm. Furthermore, our observations highlight the concept that age at injury may determine functional alterations and response to treatment.

Similar to what has been observed in kittens and in contrast to adult rats, the CAP of the uninjured immature rat was slower, had longer latencies and required more current (23, 53). Diffuse brain injury in the immature rat resulted in decreased amplitude of the CAP by 1 dpi in both unmyelinated and myelinated fibers, as has been reported for the brain-injured adult rat (23, 24). However, in contrast to the adult brain-injured rat where the amplitude of the myelinated fibers recovered to near control levels by 7 dpi (23), we observed a sustained deficit up to 2 weeks, which may suggest differences in injury severity between the two ages. Brain injury resulted in sustained deficits in the unmyelinated fibers up to 7 dpi in the adult rat and up to 14 dpi in the immature rat (23, 24), suggesting that the unmyelinated axons at either age may be more vulnerable to trauma despite potential differences in injury severity. It is important to note that midline fluid percussion injury to the adult rat brain does not result in skull fractures or hematomas, which may affect the outcome. The decrease in both the amplitude and the duration of the CAP suggest that myelinated and unmyelinated axons are either dysfunctional or that fewer axons are contributing to the CAP. In the acute post-traumatic period, the injury-induced CAP amplitude decrease may be the result of dysfunctional sodium channels, which are proteolyzed by calpain following mechanical trauma in vitro or in vivo (54, 55). The evidence of axonal degeneration over the first week post-injury suggests that the sustained deficits observed in the CAP may reflect a decreased number of axons.

Further evidence that fewer axons contribute to the CAP comes from the analyses of the conduction velocity and refractoriness. Neither the conduction velocity nor the refractoriness of the myelinated fibers was changed, suggesting that injury does not interfere with the functional properties of individual axons. In contrast, injury to the adult brain decreased the conduction velocity and increased the refractoriness of the myelinated axons (23, 27), indicating an age-at-injury response. Injury to the immature animals resulted in an increase in conduction velocity of the unmyelinated fibers that was accompanied by a decrease in the refractoriness, which may simply be the result of the greater susceptibility of the smaller axons compared to the larger axons leading to a shift in the population of unmyelinated axons. In contrast, the unmyelinated fibers in the injured adult brain exhibited decreased conduction velocity and increased refractoriness, which led the authors to conclude that the individual axons were functionally deficient (23, 27, 32, 33, 56). Structurally, axons of varying diameter exhibit different pathologic alterations post-injury, suggesting that axon caliber may contribute to traumatic susceptibility (10, 14, 57-59).

The mechanism(s) underlying CAP deficits after injury have not been completely elucidated. When the rat optic nerve was exposed to anoxic conditions ex vivo, the CAP disappeared and recovered to only 28% in the presence of Ca^{++} and 100% in Ca^{++}-free artificial cerebral spinal fluid (30). Anoxia in the presence of a calcium channel antagonist such as verapamil, diltiazem, or nifedipine resulted in greater recovery of CAP of rat optic nerves (31). Although the effect of calcium channel blockers on axonal structure and function have not been tested following TBI, the calpain inhibitor, MDL28170, and the calcineurin inhibitors, FK506 or cyclosporin A, were effective in ameliorating CAP deficits (27, 32, 33). In addition, these studies provided evidence that the calpain and calcineurin inhibitors reduced intra-axonal APP accumulation, suggesting that post-traumatic calcium entry in the adult may be associated with generalized axonal dysfunction. In contrast, we did not observe an effect of FK506 (10 and 25 mg/Kg, this report or 1 and 5 mg/Kg, data not shown) on impaired axonal transport. The doses of FK506 cannot explain this lack of an effect because lower doses were neuroprotective following CNS injury in either the adult or the immature rat (33, 46, 47, 51, 60, 61). Rather, this may reflect that in contrast to the adult rats (42-45), diffuse brain injury in the immature rat did not appear to activate calcineurin.

Calcineurin has been shown to dephosphorylate neurofilament in vitro and in vivo (40, 41). We observed intra-axonal accumulation of dephosphorylated neurofilament lending support to the idea that neurofilament compaction in the immature brain (16) may result from dephosphorylation of the side-arm domains (34-36). Although calcineurin activity did not increase after TBI, total phosphatase activity in the white matter decreased and led us to postulate that the relative contribution of calcineurin activity to the total phosphatase activity increased. This hypothesis was validated by the partial reduction of dephosphorylated neurofilament accumulations in brains of rats treated with FK506. Furthermore, the coupling of neurofilament dephosphorylation to the intra-axonal accumulation of total neurofilament suggests that disruption of axon structure may accompany axon degeneration. This was borne out by the observation that FK506 treatment reversed the post-traumatic accumulation of total neurofilament within axons and reduced axonal degeneration; the effect of FK506 and cyclosporin A on axonal degeneration in the adult rat has not been evaluated. Interestingly, the dose of FK506 that reduced axonal damage and degeneration in the immature brain-injured rat exacerbated CAP deficits at 7 dpi, suggesting that the health of the remaining axons was negatively affected by the treatment and provides additional evidence that age at injury also determines therapeutic efficacy. Alternatively, the decrease in intra-axonal SMI-32 and NF200 accumulations may suggest that FK506 treatment accelerates axonal degeneration, which may explain the decrease in the number of Fluoro-Jade B labeled profiles.

The data in the present study provide evidence of structural and functional deficits in axons of the immature brain following traumatic injury. These studies highlight the importance of using multiple outcome measures to determine efficacy of therapeutic strategies. Our observations indicate the importance of mechanistic and therapeutic studies in age-appropriate animal models of TBI.

Acknowledgments

We would like to acknowledge the efforts of Mr. David Kowalski for writing the Matlab codes that were used to analyze the electrophysiological data, and Drs. Ime Udoekwere and Corey Hart for their help with the Matlab image processing code.

These studies are supported in part by R01-HD061963 and K08-NS053651.

REFERENCES

1. Langlois JA, Rutland-Brown W, Thomas KE. The incidence of traumatic brain injury among children in the United States: differences by race. J Head Trauma Rehabil. 2005; 20:229–38. [PubMed: 15908823]
2. Coronado VG, Xu L, Basavaraju SV, et al. Surveillance for traumatic brain injury-related deaths--United States, 1997-2007. MMWR Surveill Summ. 2011; 60:1–32. [PubMed: 21544045]
3. Tong KA, Ashwal S, Holshouser BA, et al. Diffuse axonal injury in children: clinical correlation with hemorrhagic lesions. Ann Neurol. 2004; 56:36–50. [PubMed: 15236400]
4. Babikian T, Freier MC, Tong KA, et al. Susceptibility weighted imaging: neuropsychologic outcome and pediatric head injury. Pediatr Neurol. 2005; 33:184–94. [PubMed: 16139733]
5. Babikian T, Tong KA, Galloway NR, et al. Diffusion-weighted imaging predicts cognition in pediatric brain injury. Pediatr Neurol. 2009; 41:406–12. [PubMed: 19931161]
6. Buki A, Siman R, Trojanowski JQ, et al. The role of calpain-mediated spectrin proteolysis in traumatically induced axonal injury. J Neuropathol Exp Neurol. 1999; 58:365–75. [PubMed: 10218632]
7. Okonkwo DO, Pettus EH, Moroi J, et al. Alteration of the neurofilament sidearm and its relation to neurofilament compaction occurring with traumatic axonal injury. Brain Res. 1998; 784:1–6. [PubMed: 9518527]
8. Saatman KE, Bozyczko-Coyne D, Marcy V, et al. Prolonged calpain-mediated spectrin breakdown occurs regionally following experimental brain injury in the rat. J Neuropathol Exp Neurol. 1996; 55:850–60. [PubMed: 8965100]
9. Povlishock JT, Becker DP, Cheng CL, et al. Axonal change in minor head injury. J Neuropathol Exp Neurol. 1983; 42:225–42. [PubMed: 6188807]
10. Stone JR, Singleton RH, Povlishock JT. Intra-axonal neurofilament compaction does not evoke local axonal swelling in all traumatically injured axons. Exp Neurol. 2001; 172:320–31. [PubMed: 11716556]
11. Pettus EH, Povlishock JT. Characterization of a distinct set of intra-axonal ultrastructural changes associated with traumatically induced alteration in axolemmal permeability. Brain Res. 1996; 722:1–11. [PubMed: 8813344]
12. Buki A, Povlishock JT. All roads lead to disconnection?--Traumatic axonal injury revisited. Acta Neurochir (Wien). 2006; 148:181–93. discussion 93-4. [PubMed: 16362181]
13. Creed JA, DiLeonardi AM, Fox DP, et al. Concussive brain trauma in the mouse results in acute cognitive deficits and sustained impairment of axonal function. J Neurotrauma. 2011; 28:547–63. [PubMed: 21299360]
14. Jafari SS, Nielson M, Graham DI, et al. Axonal cytoskeletal changes after nondisruptive axonal injury. II. Intermediate sized axons. J Neurotrauma. 1998; 15:955–66. [PubMed: 9840768]
15. Saatman KE, Abai B, Grosvenor A, et al. Traumatic axonal injury results in biphasic calpain activation and retrograde transport impairment in mice. J Cereb Blood Flow Metab. 2003; 23:34–42. [PubMed: 12500089]

16. DiLeonardi AM, Huh JW, Raghupathi R. Impaired axonal transport and neurofilament compaction occur in separate populations of injured axons following diffuse brain injury in the immature rat. Brain Res. 2009; 1263:174–82. [PubMed: 19368848]
17. Raghupathi R, Huh JW. Diffuse brain injury in the immature rat: evidence for an age-at-injury effect on cognitive function and histopathologic damage. J Neurotrauma. 2007; 24:1596–608. [PubMed: 17970623]
18. Adelson PD, Jenkins LW, Hamilton RL, et al. Histopathologic response of the immature rat to diffuse traumatic brain injury. J Neurotrauma. 2001; 18:967–76. [PubMed: 11686497]
19. Huh JW, Widing AG, Raghupathi R. Midline brain injury in the immature rat induces sustained cognitive deficits, bihemispheric axonal injury and neurodegeneration. Exp Neurol. 2008; 213:84–92. [PubMed: 18599043]
20. Raghupathi R, Margulies SS. Traumatic axonal injury after closed head injury in the neonatal pig. J Neurotrauma. 2002; 19:843–53. [PubMed: 12184854]
21. Gennarelli TA. The spectrum of traumatic axonal injury. Neuropathol Appl Neurobiol. 1996; 22:509–13. [PubMed: 9004238]
22. Maxwell WL, Povlishock JT, Graham DL. A mechanistic analysis of nondisruptive axonal injury: a review. J Neurotrauma. 1997; 14:419–40. [PubMed: 9257661]
23. Reeves TM, Phillips LL, Povlishock JT. Myelinated and unmyelinated axons of the corpus callosum differ in vulnerability and functional recovery following traumatic brain injury. Exp Neurol. 2005; 196:126–37. [PubMed: 16109409]
24. Baker AJ, Phan N, Moulton RJ, et al. Attenuation of the electrophysiological function of the corpus callosum after fluid percussion injury in the rat. J Neurotrauma. 2002; 19:587–99. [PubMed: 12042094]
25. Ai J, Liu E, Park E, et al. Structural and functional alterations of cerebellum following fluid percussion injury in rats. Exp Brain Res. 2007; 177:95–112. [PubMed: 16924485]
26. Preston RJ, Waxman SG, Kocsis JD. Effects of 4-aminopyridine on rapidly and slowly conducting axons of rat corpus callosum. Exp Neurol. 1983; 79:808–20. [PubMed: 6825765]
27. Ai J, Liu E, Wang J, et al. Calpain inhibitor MDL-28170 reduces the functional and structural deterioration of corpus callosum following fluid percussion injury. J Neurotrauma. 2007; 24:960–78. [PubMed: 17600513]
28. Maxwell WL, Kosanlavit R, McCreath BJ, et al. Freeze-fracture and cytochemical evidence for structural and functional alteration in the axolemma and myelin sheath of adult guinea pig optic nerve fibers after stretch injury. J Neurotrauma. 1999; 16:273–84. [PubMed: 10225214]
29. Maxwell WL, McCreath BJ, Graham DI, et al. Cytochemical evidence for redistribution of membrane pump calcium-ATPase and ecto-Ca-ATPase activity, and calcium influx in myelinated nerve fibres of the optic nerve after stretch injury. J Neurocytol. 1995; 24:925–42. [PubMed: 8719820]
30. Stys PK, Ransom BR, Waxman SG, et al. Role of extracellular calcium in anoxic injury of mammalian central white matter. Proc Natl Acad Sci U S A. 1990; 87:4212–6. [PubMed: 2349231]
31. Fern R, Ransom BR, Waxman SG. Voltage-gated calcium channels in CNS white matter: role in anoxic injury. J Neurophysiol. 1995; 74:369–77. [PubMed: 7472338]
32. Colley BS, Phillips LL, Reeves TM. The effects of cyclosporin-A on axonal conduction deficits following traumatic brain injury in adult rats. Exp Neurol. 2010; 224:241–51. [PubMed: 20362574]
33. Reeves TM, Phillips LL, Lee NN, et al. Preferential neuroprotective effect of tacrolimus (FK506) on unmyelinated axons following traumatic brain injury. Brain Res. 2007; 1154:225–36. [PubMed: 17481596]
34. Hall GF, Lee VM. Neurofilament sidearm proteolysis is a prominent early effect of axotomy in lamprey giant central neurons. J Comp Neurol. 1995; 353:38–49. [PubMed: 7714248]
35. Nixon RA, Paskevich PA, Sihag RK, et al. Phosphorylation on carboxyl terminus domains of neurofilament proteins in retinal ganglion cell neurons in vivo: influences on regional neurofilament accumulation, interneurofilament spacing, and axon caliber. J Cell Biol. 1994; 126:1031–46. [PubMed: 7519617]

36. de Waegh SM, Lee VM, Brady ST. Local modulation of neurofilament phosphorylation, axonal caliber, and slow axonal transport by myelinating Schwann cells. Cell. 1992; 68:451–63. [PubMed: 1371237]
37. Saljo A, Bao F, Haglid KG, et al. Blast exposure causes redistribution of phosphorylated neurofilament subunits in neurons of the adult rat brain. J Neurotrauma. 2000; 17:719–26. [PubMed: 10972247]
38. Ma M, Matthews BT, Lampe JW, et al. Immediate short-duration hypothermia provides long-term protection in an in vivo model of traumatic axonal injury. Exp Neurol. 2009; 215:119–27. [PubMed: 18977220]
39. Chung RS, Staal JA, McCormack GH, et al. Mild axonal stretch injury in vitro induces a progressive series of neurofilament alterations ultimately leading to delayed axotomy. J Neurotrauma. 2005; 22:1081–91. [PubMed: 16238485]
40. Tanaka T, Takeda M, Niigawa H, et al. Phosphorylated Neurofilament Accumulation in Neuronal Perikarya by Cyclosporine-a Injection in Rat-Brain. Method Find Exp Clin. 1993; 15:77–87.
41. Eyer J, Leterrier JF. Influence of the phosphorylation state of neurofilament proteins on the interactions between purified filaments in vitro. Biochem J. 1988; 252:655–60. [PubMed: 2844152]
42. Kurz JE, Parsons JT, Rana A, et al. A significant increase in both basal and maximal calcineurin activity following fluid percussion injury in the rat. J Neurotrauma. 2005; 22:476–90. [PubMed: 15853464]
43. Kurz JE, Hamm RJ, Singleton RH, et al. A persistent change in subcellular distribution of calcineurin following fluid percussion injury in the rat. Brain Res. 2005; 1048:153–60. [PubMed: 15919062]
44. Bales JW, Ma X, Yan HQ, et al. Regional calcineurin subunit B isoform expression in rat hippocampus following a traumatic brain injury. Brain Res. 2010; 1358:211–20. [PubMed: 20713027]
45. Bales JW, Ma X, Yan HQ, et al. Expression of protein phosphatase 2B (calcineurin) subunit A isoforms in rat hippocampus after traumatic brain injury. J Neurotrauma. 2010; 27:109–20. [PubMed: 19751097]
46. Marmarou CR, Povlishock JT. Administration of the immunophilin ligand FK506 differentially attenuates neurofilament compaction and impaired axonal transport in injured axons following diffuse traumatic brain injury. Exp Neurol. 2006; 197:353–62. [PubMed: 16297913]
47. Singleton RH, Stone JR, Okonkwo DO, et al. The immunophilin ligand FK506 attenuates axonal injury in an impact-acceleration model of traumatic brain injury. J Neurotrauma. 2001; 18:607–14. [PubMed: 11437083]
48. Buki A, Okonkwo DO, Povlishock JT. Postinjury cyclosporin A administration limits axonal damage and disconnection in traumatic brain injury. J Neurotrauma. 1999; 16:511–21. [PubMed: 10391367]
49. Okonkwo DO, Buki A, Siman R, et al. Cyclosporin A limits calcium-induced axonal damage following traumatic brain injury. Neuroreport. 1999; 10:353–8. [PubMed: 10203334]
50. Staal JA, Dickson TC, Gasperini R, et al. Initial calcium release from intracellular stores followed by calcium dysregulation is linked to secondary axotomy following transient axonal stretch injury. J Neurochem. 2010; 112:1147–55. [PubMed: 19968758]
51. Setkowicz Z, Ciarach M, Guzik R, et al. Different effects of neuroprotectants FK-506 and cyclosporin A on susceptibility to pilocarpine-induced seizures in rats with brain injured at different developmental stages. Epilepsy Res. 2004; 61:63–72. [PubMed: 15451009]
52. Schumacher PA, Eubanks JH, Fehlings MG. Increased calpain I-mediated proteolysis, and preferential loss of dephosphorylated NF200, following traumatic spinal cord injury. Neuroscience. 1999; 91:733–44. [PubMed: 10366029]
53. Guandalini P, Franchi G, Semenza P, et al. The functional development of input-output relationships in the rostral portion of the corpus callosum in the kitten. Exp Brain Res. 1989; 74:453–62. [PubMed: 2707321]

54. Iwata A, Stys PK, Wolf JA, et al. Traumatic axonal injury induces proteolytic cleavage of the voltage-gated sodium channels modulated by tetrodotoxin and protease inhibitors. J Neurosci. 2004; 24:4605–13. [PubMed: 15140932]

55. von Reyn CR, Spaethling JM, Mesfin MN, et al. Calpain mediates proteolysis of the voltage-gated sodium channel alpha-subunit. J Neurosci. 2009; 29:10350–6. [PubMed: 19692609]

56. Reeves TM, Smith TL, Williamson JC, et al. Unmyelinated axons show selective rostrocaudal pathology in the corpus callosum after traumatic brain injury. J Neuropathol Exp Neurol. 2012; 71:198–210. [PubMed: 22318124]

57. Jafari SS, Maxwell WL, Neilson M, et al. Axonal cytoskeletal changes after non-disruptive axonal injury. J Neurocytol. 1997; 26:207–21. [PubMed: 9192287]

58. Stone JR, Walker SA, Povlishock JT. The visualization of a new class of traumatically injured axons through the use of a modified method of microwave antigen retrieval. Acta Neuropathol. 1999; 97:335–45. [PubMed: 10208272]

59. Stone JR, Okonkwo DO, Dialo AO, et al. Impaired axonal transport and altered axolemmal permeability occur in distinct populations of damaged axons following traumatic brain injury. Exp Neurol. 2004; 190:59–69. [PubMed: 15473980]

60. Nottingham S, Knapp P, Springer J. FK506 treatment inhibits caspase-3 activation and promotes oligodendroglial survival following traumatic spinal cord injury. Exp Neurol. 2002; 177:242–51. [PubMed: 12429226]

61. Wakita H, Tomimoto H, Akiguchi I, et al. Dose-dependent, protective effect of FK506 against white matter changes in the rat brain after chronic cerebral ischemia. Brain Res. 1998; 792:105–13. [PubMed: 9593846]

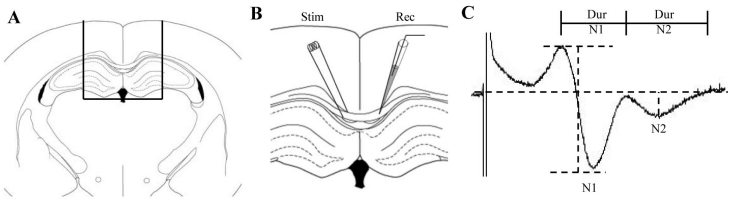

Figure 1.

Measurement of compound action potential (CAP) in the corpus callosum. (**A**) Representative schematic of the coronal slice containing the corpus callosum used for recording the CAP. (**B**) Stimulating and recording electrodes were placed approximately 0.5 mm on either side of the midline. (**C**) Representative trace of a typical CAP used to measure the amplitudes. The amplitude of the N1 component (myelinated fibers) was the difference in voltage from the first positive peak to first negative trough; the amplitude of the N2 component (unmyelinated fibers) was measured by dropping a tangent from the baseline to the second negative trough. The duration of N1 was measured as the time between the first and second positive peaks; the duration of N2 was measured as the time between the second positive peak until the signal returned to baseline.

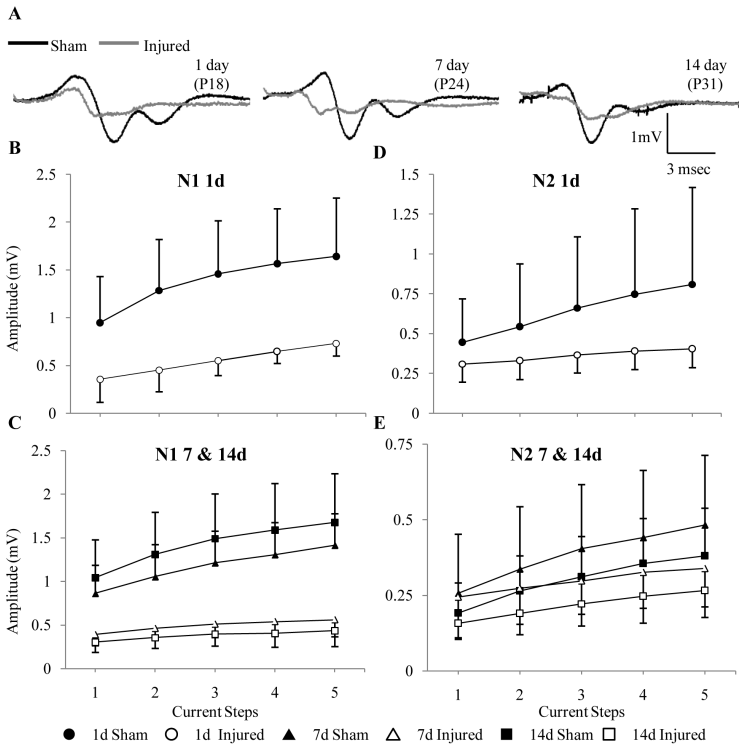

Figure 2.

Effect of diffuse brain injury on the amplitude of the compound action potentials of axons in the corpus callosum. (**A**) Representative traces from slices obtained from sham- and brain-injured at 1, 7 and 14 days following surgery/injury. (**B-E**) Input-output curves of amplitude for the N1 and N2 components at 1 (**B, D**), 7 and 14 days (**C, E**). Although the graphs are separated by time, statistical analyses were performed by combining all time points.

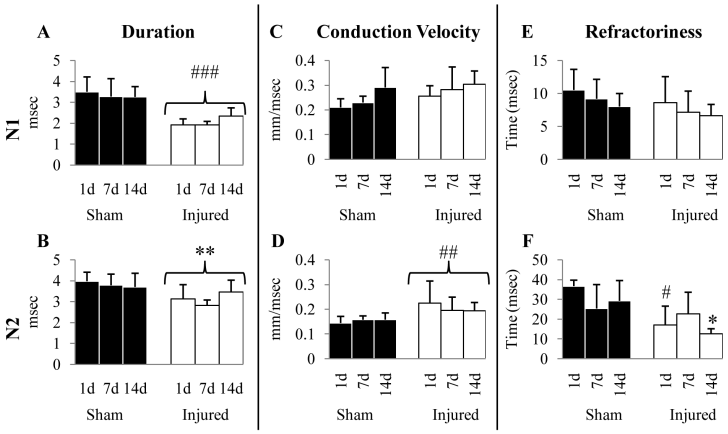

Figure 3.

Effect of diffuse brain injury on the electrophysiologic properties of the axons in the corpus callosum. (**A-F**) Graphs representing duration (**A, B**), conduction velocity (**C, D**) and refractoriness (**E, F**) of the N1 (**A, C, E**) and N2 components (**B, D, F**). Filled (sham-injured) and open (brain-injured) bars represent mean values; error bars represent SDs. All p values are significant compared to their respective sham-injured animals. *, $p < 0.05$; **, $p < 0.005$; #, $p < 0.01$; ##, $p < 0.001$; ###, $p < 0.0001$.

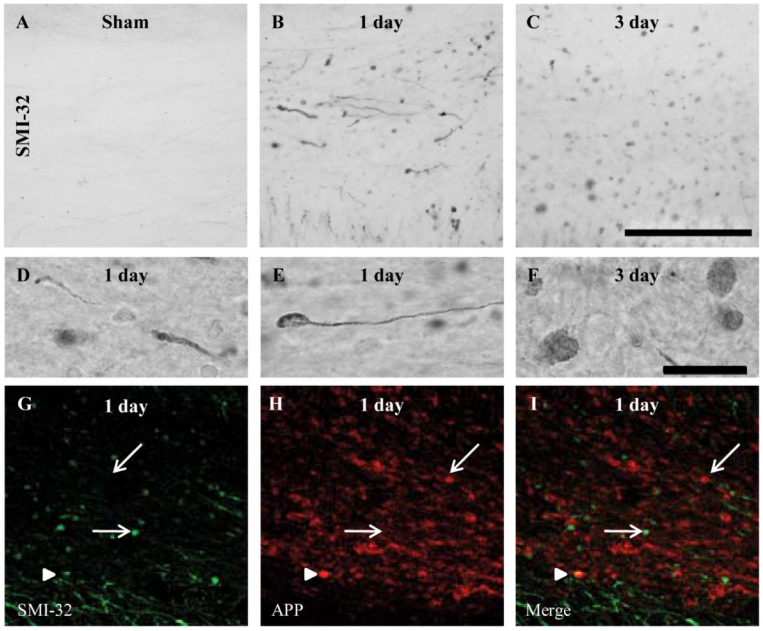

Figure 4.

Intra-axonal accumulation of dephosphorylated 200-kDa neurofilament subunit following diffuse brain injury in the immature rat. (**A-F**) Representative photomicrographs of SMI-32-labeled axons within the corpus callosum of sham (**A**), and brain-injured rats at 1 (**B**) and 3 days (**C**) post-injury. (**D**) An example of SMI-32-labeled swollen contiguous axons. (**E, F**) Examples of terminal bulbs. (**G-I**) An example of double-label immunofluorescence for intra-axonal amyloid precursor protein (APP) accumulation (red) and SMI-32 immunoreactivity (green) at 1 day post-injury. Single-labeled profiles (either APP-positive/SMI-32-negative or APP-negative/SMI-32-positive) are denoted by arrows; double-labeled profiles (APP-positive/SMI-32-positive) are denoted by arrowheads. Photomicrographs were obtained at 63x magnification. Scale bars in panels **C** (20x) and **F** (100x) represent 100 μm for panels **A-C** and **D-F**, respectively.

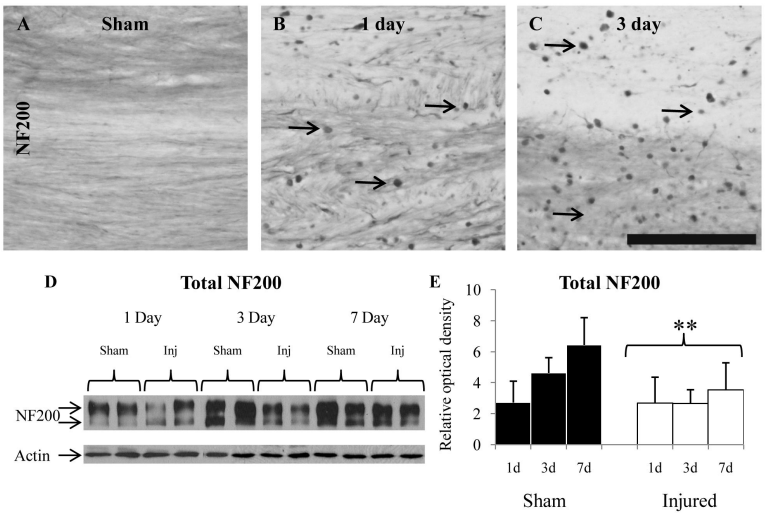

Figure 5.

Alterations in total 200-kDa neurofilament subunit (NF200) following diffuse brain injury in the immature rat. (**A-C**) Representative photomicrographs of NF200-labeled axons from a sham-injured rat (**A**), and injured rats at 1 (**B**) and 3 days (**C**) post-injury. Arrows denote examples of NF200-labeled axonal accumulation. (**D**) Representative immunoblots of NF200 and actin (loading control) using lysates of the subcortical white matter. (**E**) Quantification of the optical density of NF200 relative to that of actin. *, $p < 0.005$. Scale bar = 100 μm for all panels.

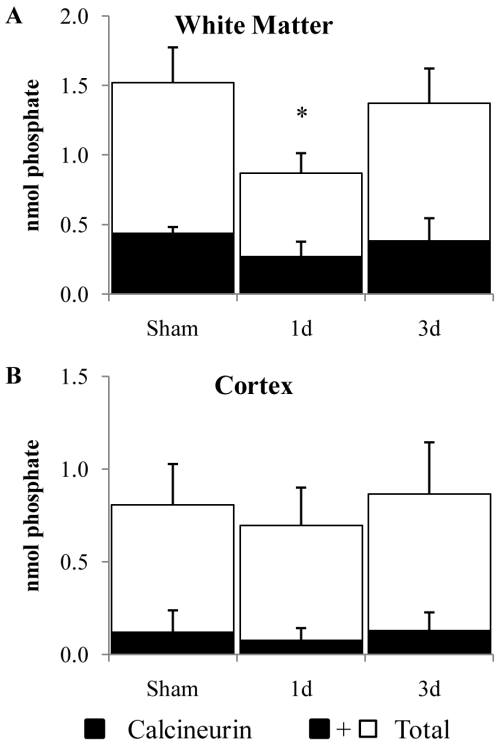

Figure 6.

Phosphatase activity following diffuse brain injury in the immature rat. (**A, B**) Total and EGTA-sensitive (calcineurin) phosphatase activities were measured using lysates of the subcortical white matter (**A**) or cortex (**B**). Shaded bars represent average calcineurin activity; the unfilled part represents average EGTA-insensitive activity. Error bars = SD. *, $p < 0.05$.

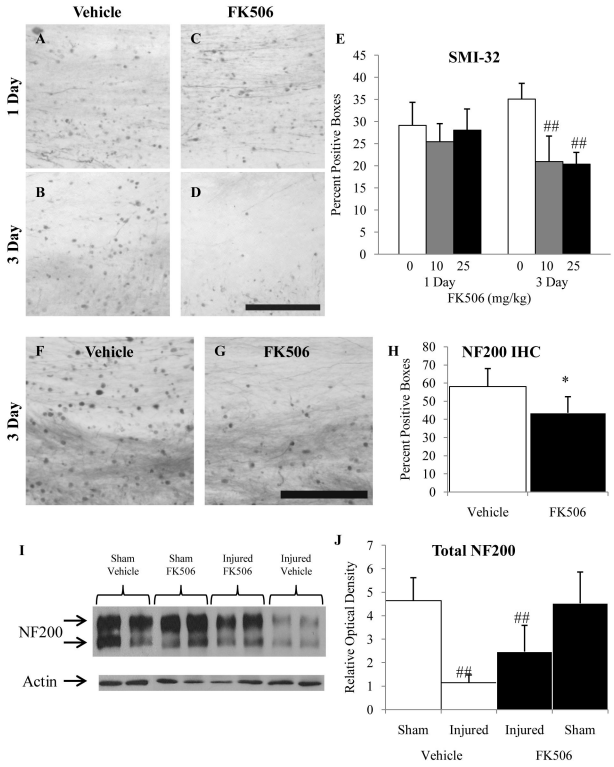

Figure 7.

Effect of FK506 on dephosphorylation and expression of 200-kDa-neurofilament subunit following diffuse brain injury in the immature rat. (**A-D**) Representative SMI-32 photomicrographs of vehicle-treated animals at 1 (**A**) and 3 (**B**) days post-injury, and FK506-treated animals at 1 (**C**) and 3 (**D**) days post-injury. E: Quantification of SMI-32-positive profiles in subcortical white matter tracts using the grid method. IHC = immunohistochemistry. (**F, G**) Representative NF200 photomicrographs of vehicle- (**F**) and FK506-treated (**G**) at 3 days post-injury. (**H**) Quantification of NF200-positive profiles in subcortical white matter tracts. (**I**) Representative immunoblots of NF200 and actin (loading control) of lysates from subcortical white matter tracts at 3 days post-injury. (**J**) Quantification of optical density of NF200 relative to that of actin. The increase in the NF200 expression in the FK506-treated injured animals was not significant. *, $p < 0.05$; ##, $p < 0.001$. Scale bar = 100 μm for all panels.

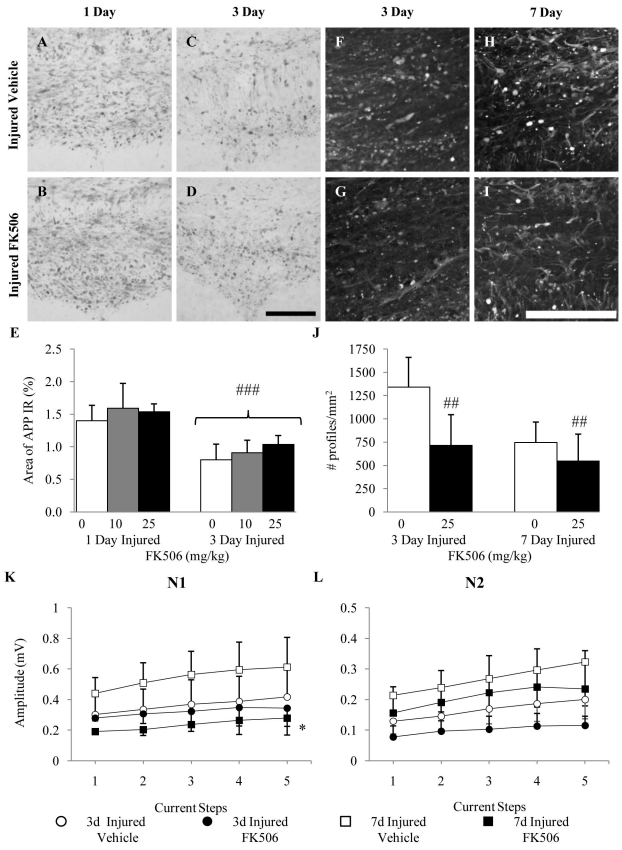

Figure 8.

Effect of FK506 on impaired axonal structure and function following diffuse brain injury in the immature rat. (**A-D**) Representative micrographs of amyloid precursor protein (APP) immunoreactivity within the corpus callosum of vehicle-treated animals at 1 (**A**) and 3 (**C**) days post-injury and FK506-treated animals at 1 (**B**) and 3 (**D**) days post-injury. (**E**) Quantification of the area of APP immunoreactivity. (**F-I**) Representative micrographs of Fluoro-Jade B (FJB) reactivity in the corpus callosum of vehicle-treated animals at 3 (**F**) and 7 (**H**) days post-injury and FK506-treated animals at 3 (**G**) and 7 (**I**) d post-injury. (**J**) Quantification of the density of FJB-positive profiles in the corpus callosum. Panels **K** and **L** illustrate the effect of vehicle or FK506 administration on the amplitude of myelinated and unmyelinated fibers, respectively, within the corpus callosum at 3 and 7 days post-injury. *, $p < 0.05$, ##, $p < 0.001$, ###, $p < 0.0001$. Scale bar = 100 μm for all panels.

Table 1

Animals for Experiments on Temporal Pattern Changes Following Diffuse Brain Injury

Outcome	Experiment	Group	Time point (d)	N	Weight (g) (mean ± SD)	Apnea (sec) (mean ± SD)
Axonal conduction	Time course	Sham	1	6	34 ± 2	NA
		Sham	7	8	33 ± 3	NA
		Sham	14	7	31 ± 3	NA
		Injured	1	8	35 ± 3	6 ± 1
		Injured	7	8	35 ± 3	7 ± 2
		Injured	14	7	33 ± 2	6 ± 1
Neurofilament dephosphorylation (Immunohistochemistry)	Time course from (19)	Sham	1	4	36 ± 2	NA
		Sham	3	4	36 ± 3	NA
		Sham	7	4	38 ± 2	NA
		Injured	1	4	35 ± 2	5 ± 0
		Injured	3	4	37 ± 2	7 ± 3
		Injured	7	4	35 ± 1	6 ± 2
Neurofilament expression (Western blots)	Time course	Sham	1	5	34 ± 4	NA
		Sham	3	4	36 ± 6	NA
		Sham	7	5	34 ± 3	NA
		Injured	1	7	38 ± 4	6 ± 1
		Injured	3	7	34 ± 4	7 ± 3
		Injured	7	7	36 ± 4	6 ± 2
Calcineurin activation	Time course	Sham	1 and 3	8	36 ± 5	NA
		Injured	1	10	35 ± 5	5 ± 2

The animals used to determine the pattern of neurofilament dephosphorylation were generated in an earlier study (19). NA = not applicable.

Table 2

Animals Used in Post-injury FK506 Treatment Experiments

Outcome	Experiment	Group	Time point (d)	N	Weight (g) (mean ± SD)	Apnea (sec) (mean ± SD)
Axonal conduction	FK506 treatment	Vehicle	3	6	36 ± 2	6 ± 1
		FK506-25	3	5	35 ± 2	6 ± 1
		Vehicle	7	5	33 ± 1	6 ± 1
		FK506-25	7	7	36 ± 1	6 ± 1
Neurofilament dephosphorylation, IAT, axonal degeneration (Immunohistochemistry and Histology)	FK506 treatment	Vehicle	1	7	38 ± 5	7 ± 2
		FK506-10	1	7	34 ± 2	7 ± 2
		FK506-25	1	6	37 ± 3	7 ± 2
		Vehicle	3	6	37 ± 4	6 ± 1
		FK506-10	3	6	34 ± 2	6 ± 1
		FK506-25	3	6	36 ± 3	6 ± 1
		Vehicle	7	6	35 ± 2	6 ± 2
		FK506-25	7	6	35 ± 2	6 ± 1
Neurofilament expression (Western blots)	FK506 treatment	Vehicle - Injured	3	4	34 ± 1	6 ± 0
		FK506-25 – Injured	3	4	34 ± 1	6 ± 1
		Vehicle – Sham	3	3	34 ± 1	NA
		FK506-25 – Sham	3	4	36 ± 6	NA

FK506-10, 10 mg/Kg FK506/injection; FK506-25, 25 mg/Kg FK506/injection; IAT, impaired axonal transport measured using intra-axonal accumulation of amyloid precursor protein. Vehicle, 20% methanol in phosphate-buffered saline.